Pyrrolobenzimidazoles Linked to Heterocycles and Peptides. Design of DNA Base Pair Specific Phosphate Hydrolyzing Agents and Novel Cytotoxic Agents

Arman Ghodousi, Xiaofen Huang, Zheng Cheng, and Edward B. Skibo*

Department of Chemistry and Biochemistry, Arizona State University, Tempe, Arizona 85287-1604

Received June 4, 2003

Work in this laboratory has been involved with the design of aziridinyl quinone-based cancer drugs (PBIs) capable of both recognizing the DNA major groove and cleaving the phosphate backbone upon reduction to the hydroquinone. The hydroquinone species recognizes the major groove of DNA at single base pairs by Hoogsteen-type hydrogen bonding. The present study extends recognition beyond a single base pair by adding amino acid residues to the 3-amino center of the PBI system. Thus, extension with proline or proline-glycine results in phosphate cleavage at 5′-AA-3′ with insignificant N(7) guanine alkylation. Molecular models were used to validate the observed sequence specificity. This report also describes the design of PBIs not capable of DNA alkylation. Removal of major groove interactions by methylation or the presence of steric bulk prevented DNA alkylation reactions upon reductive activation. From these studies it was concluded that DNA alkyation was not necessary for PBI cytostatic and cytotoxic activity. For example, linkage of two phenylalanines to the PBI results in highly selective cytostatic and cytotoxic activity against melanoma, although this compound is a weak DNA alkylator.

Previous work in this laboratory resulted in the discovery of the pyrrolo[1,2-*a*]benzimidazoles (PBIs) that are able to recognize single base pairs by Hoogsteen base pairing.[1−6] Figure 1 shows the reduced 3-amino PBI interacting with the AT base pair in the DNA major groove.[6] In this model the 3-amino group is a hydrogen-bond-donor to the thymine carbonyl, while the fused imidazo nitrogen and the hydroquinone hydroxyl are hydrogen bonded to the adenine base. As a result, the aziridinyl group is brought to within 3.3 Å of phosphate oxygen. The cutting of the DNA backbone involves alkylation of the phosphate oxygen followed by nucleophilic cleavage of the resulting phosphotriester.[2,7] The formation of the neutral phosphotriester backbone promotes hydrolytic cleavage of the DNA phosphate backbone. Similarly, lanthanum-mediated cleavage of DNA involves complexation with the anionic phosphate backbone followed by hydrolysis.[8,9] In addition, Receptors have been designed that neutralize the phosphate charge and facilitate hydrolysis.[10]

The present report explores the possibilities that the 3-substituent of the PBI will provide additional interactions in the major groove, resulting in recognition of more than one base pair, and/or assist in cellular uptake. Shown in Chart 1 are the heterocycles, amino acid, and peptide substituents linked to the PBI 3-position. The linking of peptides to antitumor agents has been carried out with variable results on antitumor activity[11−14] Linked peptides could assist in drug delivery across the cellular membrane and thereby increase activity as well as assist in DNA recognition.

Our results show that some 3-substituents increased the specificity of DNA hydrolytic cleavage, while other 3-substituents resulted in loss of all DNA interactions. Both observations were rationalized by employing molecular models. A DNA interaction is not required for cytostatic/cytotoxic activity, and in one case evidence of inhibition of IMP dehydrogenase by a PBI was obtained. The highest cytotoxic activity was observed with phenylalanine (**1l**) and phenylalanine-phenylalanine (**1m**) linked PBIs, presumably due to an active uptake process.

Results and Discussion

The PBI Analogues Studied and Their Synthesis. The extended PBI compounds prepared for this study are shown in Chart 1. The choice of these particular substituents was based on the following considerations. Attachment of the pyridine substituents to the PBI system, as in **1a**−**c**, could provide additional hydrogen-bonding interactions in the major groove, resulting in two-base-pair recognition. On the other hand, the bulky quinoline of **1d** and the alkyl substituents of **1e** and **1f** should preclude DNA binding altogether. The study of **1d**−**f** would therefore provide an assessment of cytotoxicity unrelated to DNA alkylation and cleavage. Finally, the amino acid and peptide derivatives **1g**−**n** could provide multiple hydrogen bonding and van der Waal interactions that would result in recognition of multiple base pairs. Insights into substituent−major groove interactions were made by attaching the substituents to a model of DNA-bound PBI (Figure 1) and then minimizing the new structures. Besides DNA recognition, we were also concerned with entry of the linked PBI into a cell. Since phenylalanine analogues are actively taken up into cancer cells,[15−17] the phenylalanine-linked PBI analogues **1l**−**n** were prepared to facilitate cellular uptake.

PBI analogues shown in Chart 1 were either prepared as racemates or pure enantiomers. The *R*- and *S*-enantiomers of PBIs possess different cytotoxicity and DNA base pair specificity,[5,6] and therefore, *S*-(−)- and *R*-(+)-**1c** were prepared for comparative studies. Both

* Corresponding author. Tel: (480) 965-3581. Fax: (480) 965-2747. E-mail: Eskibo@asu.edu.

10.1021/jm0302750 CCC: $27.50
Published on Web 11/26/2003

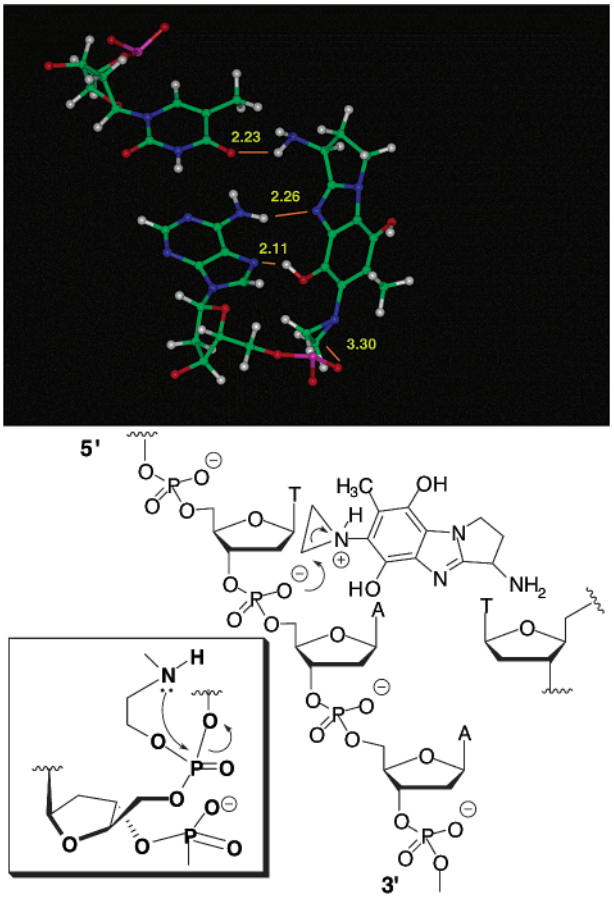

Figure 1. Molecular model of reduced 3-amino PBI in the major groove of an AT base pair showing hydrogen-bonding interactions and the aziridinyl group proximal to phosphate. The mechanisms of the alkylation and cleavage processes are shown below the model.

the *R*- and *S*-enantiomers of 3-amino PBI (**2**) were prepared previously,[5] and DCC coupling of either enantiomer with isonicotinic acid afforded enantiomers of **1c**. Racemic forms of **1a**,**b**,**d**−**f** were prepared by DCC coupling of the appropriate acid to racemic 3-amino PBI (**2**), which was prepared as shown in Scheme 1. The preparation of the *S*-enantiomers of **2g**−**k** was carried out starting with the *S*-enantiomer of the 3-aminopyrrolobenzimidazole (Scheme 1).[5,18] DCC-mediated coupling of a tBOC-protected amino acid to this amine group, followed by removal of the tBOC with trifluoroacetic acid (TFA), afforded amino acid linked PBI. At this point, the amino acid could be extended further by treatment with another tBOC-protected amino acid and DCC to afford a dipeptide or converted to the aziridinyl quinone form.

DNA Alkylation and Cleavage. Assessments of DNA reductive alkylation by PBI analogues were made by measuring the percent incorporation of the blue aminoquinone chromophore into DNA as well as measuring cleavage patterns with PAGE. The aminoquinone chromophore is the result of nucleophile-mediated opening of the aziridine ring of the hydroquinone followed by oxidative workup of the reaction. Measurement of the absorbance of this blue chromophore has been used as an estimate of the compound's ability to interact with DNA upon reductive activation.[2,5,19] The DNA target nucleophile of reductively activated PBIs is typically the

Chart 1

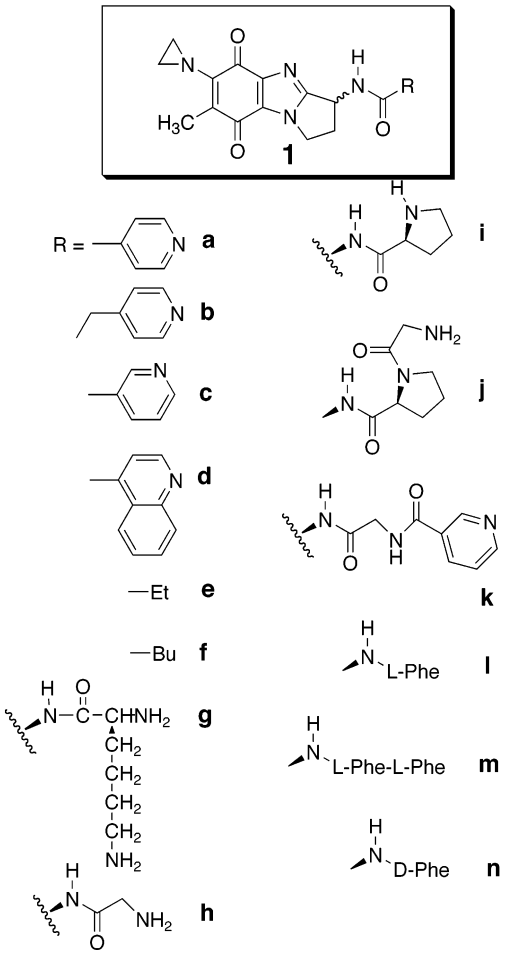

phosphate backbone.[2] However, the PBI 3-substituent could alter the interactions with DNA, resulting in N(7) guanine alkylation products typically seen with other aziridinyl quinones. A mixture of N(7) and phosphate alkylation by a reduced PBI was considered to be evidence of nonspecific DNA interactions in the present study.

The presence of phosphate alkylation was assessed from PAGE analysis of cleavage patterns obtained when the treated DNA was hydrolyzed in buffer under anaerobic conditions.[2] The phosphotriester causes backbone cleavage by the process illustrated in Figure 1, resulting in a "hydrolytic" cleavage ladder. The N(7) guanine alkylation sites were detected by employing piperdine-mediated cleavage.[20] The differentiation of purine base alkylation and phosphate backbone alkylation in this way has been utilized to study new DNA-recognition agents.[21]

Table 1 shows the DNA alkylation results for the PBIs in Chart 1 as well as that of two previously reported analogues (3-amino and *N*,*N*-dimethylcarbamido PBIs[5,6]). The sequence specificity and alkylation site [phosphate backbone or N(7) center] is also provided in this table. The nicotinic acid amide derivative **1a** shows the highest DNA percent alkylation and cut DNA hydrolytically at 5′-AA-3′, whereas **1b**−**f** are strong to weak N(7) alkylating agents. The 3-amino PBI is an efficient DNA cutter at AT base pairs, particularly at AT runs, utilizing the Hoogsteen-type hydrogen bonding shown in Figure 1. In contrast, the 3-*N*,*N*-dimethylcarbamido

Scheme 1

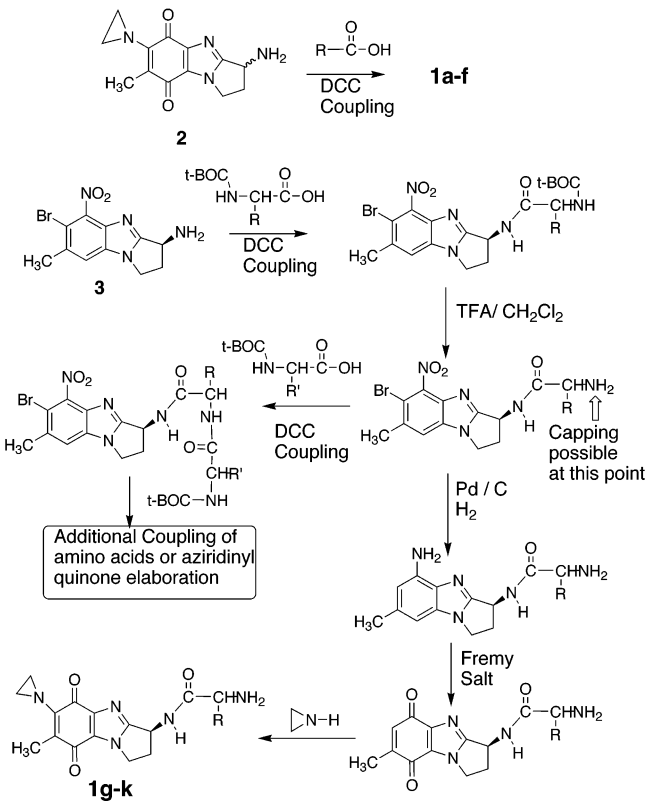

Table 1. Bulk DNA Alkylation, PAGE Sequence Specificity, and Alkylation Site of the PBIs in Chart 1

compd	% DNA alkylation[a]	sequence specificity	alkylation site
1a	79	5′-AAT-3′	phosphate
1b	35	G (strong)	N(7)
1c	20	G (weak)	N(7)
1d	10	G (weak)	N(7)
1e	∼0	G (weak)	N(7)
1f	9	G (weak)	N(7)
3-amino PBI	∼100	A-runs	phosphate
N,*N*-Me$_2$-carbamido	0	none	none
1g	−	5′-AA-3′	phosphate
		5′-GG-3′	phosphate
		G	N(7)
1h	−	5′-AA-3′	phosphate
		G	N(7)
1i	−	5′-AA-3′	3A phosphate
1j	−	5′-AA-3′	3A phosphate
		G (weak)	N(7)
1k	−	none	none
1l	−	G (weak)	N(7)
1m	−	G (very weak)	N(7)
1n	−	G (weak)	N(7)

[a] Percent bulk DNA alkylation values were not determined for amino acid PBIs (**1g**−**n**).

PBI does not alkylate DNA, even at the high concentrations found in bulk experiments.

The PAGE gel for the reduced *R*- and *S*-enantiomers of **1a** is shown in Figure 2. The *R*-enantiomer displayed weak hydrolytic cleavage (lanes 2 and 3) compared to the *S*-enantiomer (lanes 5 and 6). Both enantiomers displayed only weak N(7) alkylation-mediated cleavage (lanes 4 and 7). The 5′-AA-3′ sequence specificity observed with (*S*)-**1a** is likely the result of reduced **1a** interacting with both AT pairs rather than isolated AT pairs. Inspection of Figure 2 in fact reveals the absence of hydrolytic cleavage at isolated AT base pairs. The

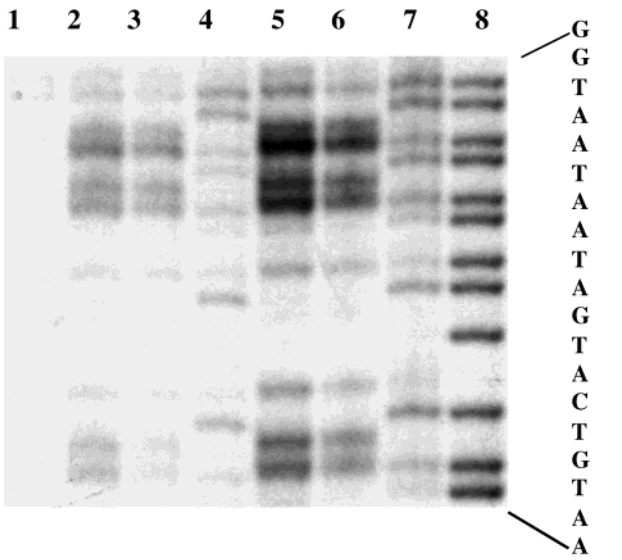

Figure 2. Autoradiogram of the induced cleavage by reduced (*R*)- and (*S*)-**1a** of a 5′-^{32}P-end-labeled 514-bp restriction fragment from pBR322 DNA (*Eco*R I/*Rsa* I). All reactions contained 10 mM Tris buffer (pH 7.4) and 50 μM DNA nucleotide (calf thymus). Lane 1, intact DNA. Lane 2, 250 μM (*R*)-**1a**, 1 mM $Na_2S_2O_4$. Lane 3, 250 μM (*R*)-**1a**, 1 mM $Na_2S_2O_4$, NaOH treatment. Lane 4, 250 μM (*R*)-**1a**, 1 mM $Na_2S_2O_4$, 0.2 mM piperidine treatment. Lane 5, 250 μM (*S*)-**1a**, 1 mM $Na_2S_2O_4$. Lane 6, 250 μM (*S*)-**1a**, 1 mM $Na_2S_2O_4$, NaOH treatment. Lane 7, 250 μM (*S*)-**1a**, 1 mM $Na_2S_2O_4$, 0.2 mM piperidine treatment. Lane 8, Maxam−Gilbert A+G reactions.

model in Figure 3 shows postulated interactions between reduced (*S*)-**1a** and the AT base pairs, with the aziridinyl center covalently bound to the phosphate responsible for the major hydrolytic cleavage band. In this model, the PBI portion of reduced (*S*)-**1a** binds to the A base as illustrated for the 3-amine PBI in Figure 1. Hydrogen bonding between PBI amide NH of (*S*)-**1a** and the adjacent adenine amine in the 5′-direction results in the observed sequence specificity. In addition to these interactions, the hydroxyl group of the reduced PBI is a hydrogen-bond donor to the phosphate backbone, and the pyridyl group undergoes a hydrophobic interaction with the thymine methyl group. Consistent with this model, reduced (*R*)-**1a** displayed only weak 5′-AA-3′ cleavage due to the change in position of the amide NH. The importance of the position of the nicotinic acid nitrogen was apparent from the PAGE gels (not shown) of the *m*-nicotinic acid (**1c**), which lost all hydrolytic cleavage specificity and exhibited only N(7) alkylation-mediated cleavage. It appears from the model shown in Figure 3 that the pyridyl nitrogen of **1a** does not contribute to DNA recognition. In fact, the absence of this nitrogen (the benzamido derivative) does not change the sequence specificity. The change in sequence specificity exhibited by the *m*-nicotinic acid (**1c**) could be due to the presence of other interactions with DNA that prevent the alkylation of phosphate.

Inspection of the PAGE in Figure 2 reveals apparent cleavage at the T-base in the 3′-direction from the 5′-AA-3′ sequence. The reduced PBI cannot bind to the TA base pair due to steric hindrance with the thymine methyl group. The explanation is the presence of two modes of phosphate hydrolysis, one of which gives rise to "A-cleavage" (inset of Figure 3), the same band as that produced by Maxam and Gilbert A-cleavage. The

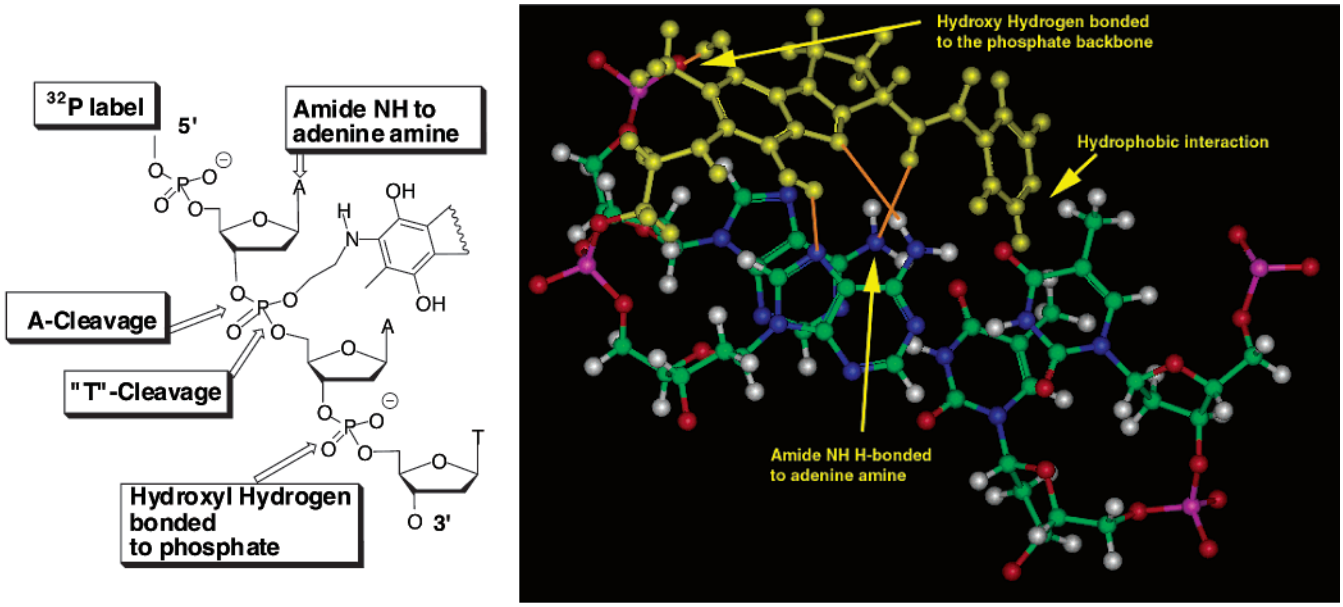

Figure 3. Molecular model of reduced (*S*)-**1a** in the major groove of 5′-AA-3′ with binding interactions labeled. The site of alkylation and the two possible cleavage products are shown in the inset.

other mode of phosphate triester cleavage will result in the PBI fragment attached to the labeled piece of DNA. This band will move somewhat slower than the A-cleavage band and give the appearance of "T-cleavage."

The presence of bulky or lipophilic substituents in **1d**−**f** caused a substantial decrease in bulk DNA reductive alkylation (Table 1). The presence of alkyl bulk in **1d**−**f**, as opposed to the flat pyridine ring of **1a**, interferes greatly with binding to the major groove. In fact, a model of the 3-*N*,*N*-dimethylcarbamido PBI shows that the major groove interaction illustrated in Figures 1 and 3 are prohibited. Nonalkylating PBIs provided an assessment of the role of DNA alkylation on cytotoxicity (see Cytostatic and Cytotoxic Properties).

Table 1 also lists the DNA reductive alkylation and cleavage results for the amino acid-linked PBIs shown in Chart 1. PAGE was used to determine the sequence and type of cleavage (phosphate versus N-7-cleavage) as well as the sequence specificity of these analogues.

The reduced lysine linked analogue **1g** underwent phosphate cleavage at 5′-AA-3′ and 5′-GG-3′, while N-7-cleavage was most prominent at 5′-GG-3′ (Figure 4). The lysine amine will be protonated at the pH of the experiment (pH 7.4) and could undergo an electrostatic interaction with the anionic phosphate backbone. The model shown in Figure 5 in fact shows that the side chain amine of lysine could reach the phosphate backbone and the α-amino group could hydrogen bond to the adjacent AT base pair (to the adenine amine or the thymine carbonyl), resulting in the observed 5′-AA-3′cleavage specificity. The apparent cleavage at both bases of 5′-AA-3′ is likely the result of phosphotriester hydrolysis at both the 3′- and the 5′-directions (see the inset of Figure 3).

To facilitate recognition of 5′-AA-3′, investigations were carried out with glycine-, proline-, and Pro-Gly-linked PBIs. The α-amino group (neutral or protonated) of the glycine of **1h** or proline of **1i** was intended to assist in recognition of 5′-AA-3′ by hydrogen bonding to the adjacent AT base pair. Cleavage studies revealed that reduced **1h** exhibited hydrolytic cleavage specificity

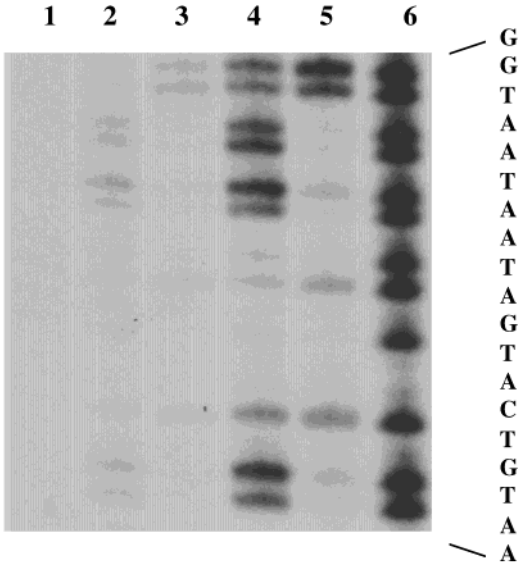

Figure 4. Autoradiogram of induced cleavage by reduced **1g** of a 5′-^{32}P-end-labeled 514-bp restriction fragment from pBR322 DNA (*Eco*R I/*Rsa* I). All reactions contained 10 mM Tris buffer (pH 7.4) and 50 μM DNA nucleotide (calf thymus). Lane 1, intact DNA. Lane 2, 1.25 μM **1g**, 1 mM $Na_2S_2O_4$. Lane 3, 1.25 μM **1g**, 1 mM $Na_2S_2O_4$, 0.2 mM piperidine treatment. Lane 4, 5 μM **1g**, 1 mM $Na_2S_2O_4$. Lane 5, 5 μM **1g**, 1 mM $Na_2S_2O_4$, 0.2 mM piperidine treatment. Lane 6, Maxam−Gilbert A+G reactions.

(at both phosphates of 5′-AA-3′) but still alkylated at guanine N(7) sites, PAGE not shown. The turn produced by the proline of **1i** was predicted to improve major-groove recognition and phosphate cleavage based on molecular modeling. In fact, the proline-linked analogue **1i** cleaved largely at the 3′-A of the sequence 5′-AA-3′, without apparent N(7)-guanine alkylation (Figure 6). The molecular model shown in Figure 7 shows the four hydrogen bonds that could result in recognition and hydrolytic cleavage at this base. The presence of proline, rather than the flexible lysine, results in cleavage largely at the 3′-A of the sequence 5′-AA-3′. Coupling of glycine to **1i** to afford **1j** resulted in the return of some

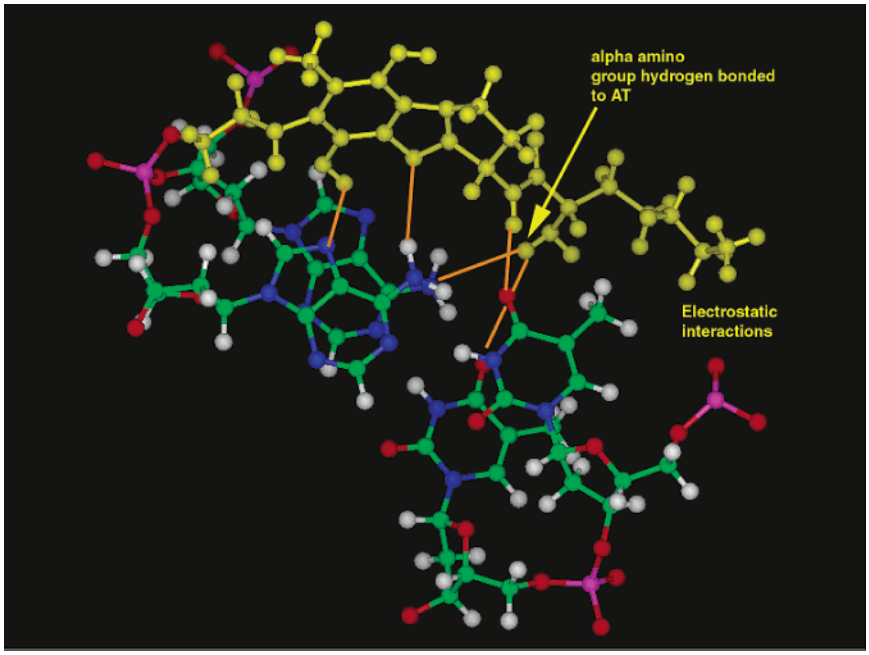

Figure 5. Molecular model of reduced **1g** in the major groove of 5′-AA-3′ with binding interactions labeled.

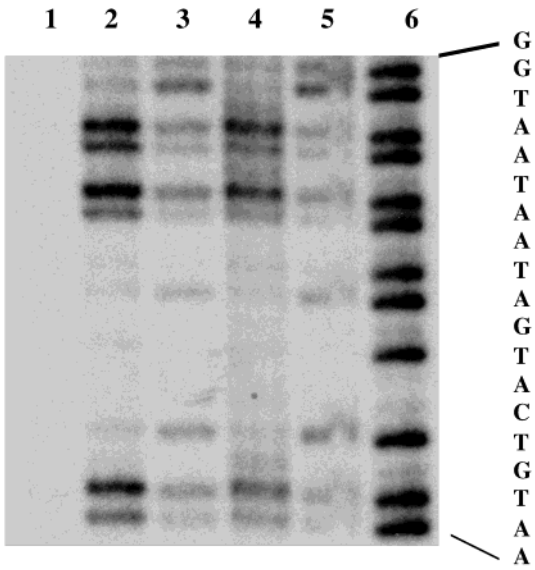

Figure 6. Autoradiogram of the cleavage by reduced **1i** of a 5′-^{32}P-end-labeled 514-bp restriction fragment from pBR322 DNA (*Eco*R I/*Rsa* I). All reactions contained 10 mM Tris buffer (pH 7.4) and 40 μM DNA nucleotide (calf thymus). Lane 1, intact DNA. Lane 2, 100 μM **1i**, 1 mM $Na_2S_2O_4$. Lane 3, 100 μM **1i**, 1 mM $Na_2S_2O_4$, 0.2 mM piperidine treatment. Lane 4, 400 μM **1i**, 1 mM $Na_2S_2O_4$. Lane 5, 400 μM **1i**, 1 mM $Na_2S_2O_4$, 0.2 mM piperidine treatment. Lane 6, Maxam−Gilbert A+G reactions.

N(7)-guanine alkylation with major cleavage at the 3′-A phosphate of 5′-AA-3′.

PBIs linked to capped glycine and phenylalanine (**1k**−**1n**) afforded analogues that are capable of utilizing lipophilicity or uptake mechanisms to gain entry into cells. In addition, addition of the bulk resulted in poor reductive alkylating agents of DNA. The phenylalanine-linked PBI (**1l**) reductively alkylated DNA only at guanine N(7)-position while the Phe-Phe linked PBI (**1m**) did so only weakly.

Cytostatic and Cytotoxic Properties. Provided in Table 2 are the cytostatic/cytotoxic parameters and cancer specificities for select PBI analogues **1**. The cytostatic parameters include GI_{50} and TGI, which are the concentrations of drug required for 50% growth inhibition and total growth inhibition, respectively. The cytotoxic parameter is the LC_{50}, which is the concentration required for 50% cell kill. These in vitro data were obtained under the In Vitro Cell Line Screening Project at the National Cancer Institute.[22,23] The log mean values for GI_{50}, TGI, and LC_{50} in 60 cell lines are provided in Table 2 along with the log Δ value (the maximum sensitivity in excess of the mean) and the log range (the maximum difference between the least sensitive and the most sensitive cell lines). These parameters provided insights into selectivity and potency of antitumor agents.[19] Large values of the Δ and range indicate high selectivity for some histological cancers over others.

The cytostatic and cytotoxic properties of **1a** were compared with those of 3-*N*,*N*-dimethylcarbamido PBI, because they represent extremes in DNA alkylation capabilities: **1a** is the best alkylating agent in Table 1, while the 3-*N*,*N*-dimethylcarbamido analogue is the worst. On the other hand, both compounds are substrates for DT-diaphorase. The human DT-diaphorase specificity of both enantiomers of the 3-*N*,*N*-dimethylcarbamido analogue ($k_{cat}/K_m = 9.4$ and 21.3×10^{-5} M^{-1} s^{-1}) was studied in conjunction with active site computer modeling.[24] Measurement of the human DT-diaphorase specificity of **1a** revealed a similar substrate specificity, $k_{cat}/K_m = 33 \times 10^{-5}$ M^{-1} s^{-1}. The data in Table 2 indicate that **1a** and the carbamido derivative have nearly identical cytostatic and cytotoxic parameters. Melanoma is the histological cancer most sensitive to both compounds and is largely responsible for the observed Δ values. Both compounds are inactive against leukemias, resulting in a parameter range of nearly 3 orders of magnitude. The parameters for individual cell lines are nearly identical for **1a** and the carbamido derivative, and the results obtained with both compounds against the melanoma panel are provided in Figure 8.

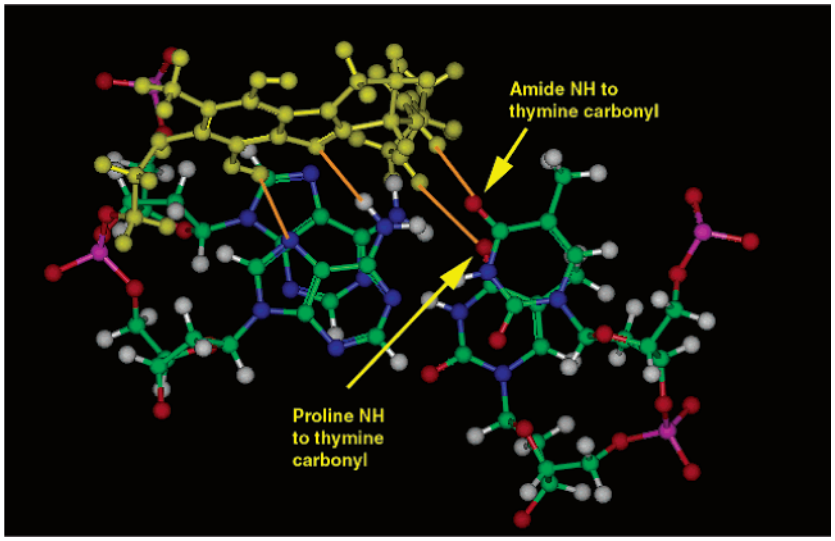

Figure 7. Molecular model of reduced **1i** in the major groove of 5′-AA-3′ with binding interactions labeled.

Table 2. Cytostatic and Cytotoxic Parameters for Amino Acid-Linked PBIs

	GI_{50}			TGI			LC_{50}		
compd	median	D	range	median	D	range	median	D	range
1a	−6.84	0.94	1.96	−6.21	1.14	2.50	−5.37	1.11	2.35
N,*N*-Me_2 carbamido	−6.97	0.96	2.73	−6.91	1.26	3.12	5.42	1.18	2.30
1i	−6.54	1.46	3.34	−5.72	1.08	2.80	−4.74	1.53	2.27
1l	−7.87	0.13	1.69	−6.61	1.39	4.00	−4.72	3.28	4.00
1m	−7.84	0.16	2.42	−7.15	0.85	4.00	−5.39	2.61	4.00
1n	−7.10	0.65	2.30	−6.29	1.06	3.34	−5.16	1.71	2.87

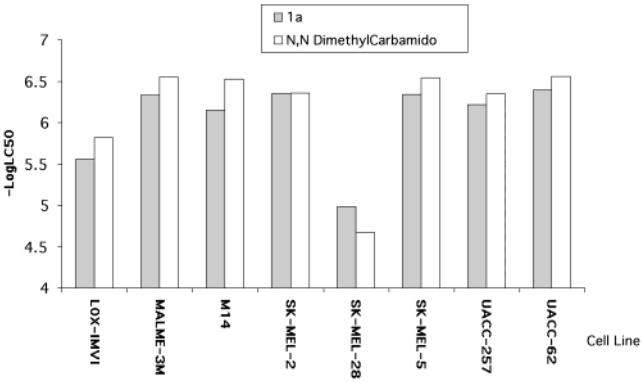

Figure 8. Comparative cytotoxicity of **1a** and the *N*,*N*-dimethylcarbamido-PBI against human melanoma cell lines.

These results indicate that DNA alkylation must not be responsible for the cytostatic/cytotoxic properties of both **1a** and the carbamido derivative. COMPARE analysis provided insights into what the molecular target might be.[22,25] The pattern of cytostatic and cytotoxic parameters (GI_{50}, TGI, and LC_{50} mean graphs) of **1a** and the *N*,*N*-dimethylcarbamido derivative was compared with those of over 38 000 compounds in the National Cancer Institute's archives. The goal was to find a compound of known mechanism of action that correlated well with the mean graphs of both compounds. The IMP dehydrogenase inhibitor NSC number 621959[26] shown in Chart 2 correlated well (nearly 0.7 correlation coefficient) with both **1a** and the *N*,*N*-dimethylcarbamido analogue. Compound 621959 is a stable analogue of NAD, and a crystal structure revealed that it occupies the binding site of the cofactor on IMP dehydrogenase.[26] Stable analogues of the NAD cofactor

Chart 2

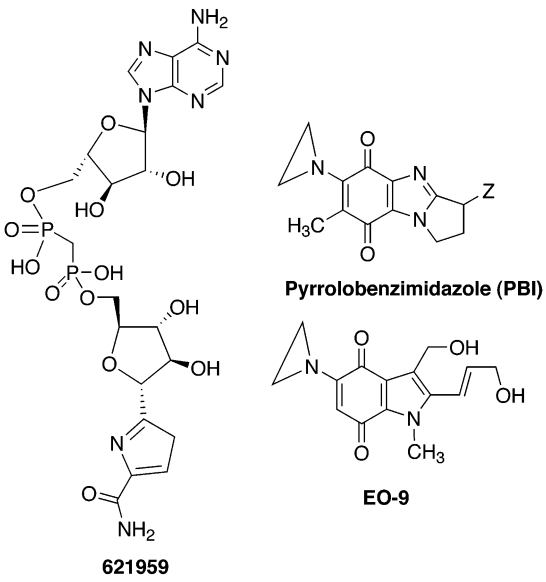

have been developed as IMP dehydrogenase inhibitors.[27−29] The cytostatic and cytotoxic activity observed for inhibitors of IMP dehydrogenase arise from the key role of this enzyme in purine metabolism and, hence, cell growth and differentiation.[30] The benzimidazole ring of **1a** and the *N*,*N*-dimethylcarbamido analogue must mimic the purine ring of NAD. In fact, benzimidazole-based IMP dehydrogenase inhibitors have been reported in the past year.[31−33]

The amino acid-linked PBIs possessed no cytostatic/cytotoxic activity (LC_{50}, TGI, and $GI_{50} > 10^{-4}$ M) except for the proline- (**1i**) and phenylanine-linked analogues (**1l**−**n**). The results of the proline-linked analogue **1i**

indicate some degree of cancer specificity with log Δ values greater than 1 (greater than 10-fold sensitivity in excess of the mean) for all parameters (Table 2). Histologic specificity is most apparent in the LC_{50} mean graph, which shows that melanoma cell lines are most sensitive to **1i**. COMPARE analysis of mean graph data revealed that **1i** has a cytostatic and cytotoxic profile unlike any known antitumor agent. The unique COMPARE could be due to a number of factors: an active uptake process combined with DT-diaphorase activation and action at a molecular target, perhaps DNA. Active uptake of proline by cancers and normal tissues has been reported,[34−36] and the proline-linked PBI could be taken up as well. The absence of active uptake is likely the main reason amino acid-linked PBIs **1h**, **1j**, and **1k** lack activity, since these compounds are capable of cleaving DNA and should therefore be cytotoxic.

The phenylalanine-linked analogue **1l** possessed both high cytostatic and cytotoxic activity along with high cancer selectivity in some mean graphs. The GI_{50} mean graph of **1l** revealed the slight selectivity (log Δ only 0.13) with log $GI_{50} < -8$ for most cell lines, but the TGI mean graph revealed selectivity against NSC lung, colon, melanoma, and renal cancers (log $\Delta = 1.26$). The 4 order of magnitude range of activity reflects the absence of activity against leukemia (log TGI > -4.00) and the high activity against melanoma (log TGI < -8). The LC_{50} mean graph for **1l** revealed very high selectivity against NSC lung, colon, melanoma, and renal cancers (log $\Delta = 3.28$). Addition of another phenylalanine (**1m**) resulted in increased cytotoxic and cytostatic activity over **1l**, with the distinguishing feature of high cytotoxic selectivity against only the melanoma cell lines (log $\Delta = 2.61$). The activity of the phenylalanine-linked PBIs could be related to active uptake mediated by the L-amino acid transporter.[37] To test the importance of L-amino acid transport, the unnatural D-phenylalanine enantiomer was linked to the PBI to afford **1n**. Consistent with L-amino acid transport, **1n** displayed significantly higher mean GI_{50} and TGI values than **1l**. The most significant difference is the loss of cancer selectivity in the LC_{50} mean graph: log Δ decreases from 3.28 to 1.71 upon the change to the unnatural enantiomer. However, **1n** is not devoid of cytostatic and cytotoxic activity, and the lipophilic phenylalanine residue must facilitate entry of this analogue into the cell.

COMPARE analysis of **1i**, **1n**, and **1m** revealed no correlation with any known antitumor agent. The unique specificity of **1m** for melanoma could represent phenylalanine uptake specific for melanocytes.[38] The uptake of phenylalanine is the first step in the process of melanogenesis by these cells. However, COMPARE analysis of **1l** revealed that its cytotoxicity (LC_{50}) profile correlated (∼0.8) with the aziridinyl indoloquinone EO-9, an antitumor agent known to be reductively activated by DT-diaphorase.[39,40] Thus, **1l** has the cytotoxic properties typical of the PBIs, suggesting the presence of reductive activation by DT-diaphorase and alkylation of DNA.

Conclusions

This report describes the design of sequence-specific DNA-cleaving agents operating by hydrolytic cleavage of the phosphate backbone. The PBI system cleaves at the AT base pair upon reductive activation,[6] and the extension of the PBI system at the 3-amino center permits recognition at an additional base pair. Thus, extension with proline **1i** or proline/glycine **1j** results in phosphate cleavage at 5′-AA-3′ with insignificant N(7)-guanine alkylation. Molecular models were used to validate the observed sequence specificity. The turn produced by the proline residue is largely responsible for the two-base pair recognition. Further extension off the proline residue should permit multibase recognition.

The utility of peptide-linked PBIs as cytostatic/cytotoxic agents (and eventually antitumor agents) relies on their ability to enter cells. Not every PBI-based DNA-cleaving agent possesses cytoststic/cytotoxic activity, perhaps due to the lack of cellular uptake. The proline-linked PBI **1i** is the only phosphate hydrolytic cleaving agent exhibiting in vitro activity. The phenylalanine-linked PBI **1l** reductively alkylates at guanine N(7) and exhibits in vitro activity typical of simple PBIs.

This report also describes the design of PBIs not capable of DNA alkylation. Removal of major-groove interactions by methylation or the presence of steric bulk prevented DNA alkylation reactions upon reductive activation. In this way it was possible to assess the contribution of DNA alkylation to the cytostatic/cytotoxic mechanisms of PBIs. From these studies, it was concluded that DNA alkyation was not necessary for PBI cytostatic and cytotoxic activity. Both **1a** and the *N*,*N*-dimethylcarbamido-linked PBI appear to be NAD analogues that interact with IMP dehydrogenase. Linkage of two phenylalanines to the PBI results in highly selective cytostatic and cytotoxic activity against melanoma, although this compound is a weak DNA alkylator. Utilization of a phenylalanine uptake process specific for melanocytes could be responsible for this specificity.

Experimental Section

All analytically pure compounds were dried under high vacuum in a drying pistol over refluxing methanol. Fremy's salt was purchased from Aldrich and stored over calcium chloride desiccant in a refrigerator. Elemental analyses were run at Atlantic Microlab, Inc., Norcross, Ga. Melting points and decomposition points were determined with a Mel-Temp apparatus. All TLCs were performed on silica gel plates using a variety of solvent systems and a fluorescent indicator for visualization. IR spectra were taken as KBr pellets and only the strongest absorbances were reported. ^{1}H NMR spectra were obtained with a 300 MHz spectrometer. All chemical shifts are reported relative to TMS. Optical rotations were taken on a Perkin-Elmer polarimeter employing a 10 cm quartz cell. Kinetic studies were carried out using an OLIS-14c program. All solutions and buffers for DNA studies were prepared with doubly distilled water. Altus 20 CLEC catalyst was purchased from Altus Biologics Inc.

Compound **1n** analysis showed the percent H found to be 0.5% lower than percent H calculated. However, ^{1}H NMR spectroscopic analysis and TLC revealed a pure compound.

DNA Incorporation Studies. DNA alkylation studies were done as follows: 33 mg (0.05 mmol) of calf thymus DNA was dissolved in a mixture of 2.0 mL of double distilled water and 2.0 mL of 0.1 M pH 7.4 Tris HCl buffer and 1−2 mg of 5% palladium on activated charcoal. To this solution was added 0.004 mmol of the drug dissolved in 0.2 mL of DMSO. The resulting solution was sealed and degassed under argon for 15 min, after which the mixture was purged with H_2 until it was colorless. The solution was then purged with argon for 15 min and placed in a 30 °C water bath for 24 h. The reaction was opened to the air, and the catalyst was filtered off. To this solution was added two volumes of ethanol and 300 μL of

ammonium acetate. The mixture was chilled at −20 °C for 16 h and the DNA pellet collected by centrifuging at 12 000 rpm for 20 min. The pellet was redissolved in water and then precipitated and centrifuged again. The resulting pellet was suspended in ethanol, centrifuged, and dried. The dried pellet was weighed and dissolved in 1 mL of double distilled water, resulting in a clear solution with $\lambda_{max} \sim 550$ nm, $\epsilon \sim 750$ M^{-1} cm^{-1}. This is the chromophore of the aminoquinone resulting from nucleophile-mediated opening of the aziridine ring.

The preparation of achiral 3-amino-6-aziridinyl-7-methylpyrrolo[1,2-*a*]benzimidazole-4,7-dione(2) was carried out starting with 7-methylpyrrolo[1,2-*a*]benzimidazol-3-one,[5] which was converted to 3-hydroxylimine-2,3-dihydro-7-methyl-1*H*-pyrrolo[1,2-*a*]benzimidazole using the following procedure: 1.0 g of 7-methylpyrrolo[1,2-*a*]benzimidazol-3-one was dissolved in a mixture of 40 mL of ethanol and 20 mL of pyridine, followed by addition of 0.92 g of hydroxylamine hydrochloride. The resulting reaction mixture was stirred at room temperature for 12 h. The solvent was evaporated under reduced pressure and the solid residue was washed with water to remove the pyridinium salt. The solids were recrystallized from chloroform/hexane: 1.0 g (92% yield); mp 260−261 °C dec; TLC [butanol/water/acetic acid (5:3:2)] $R_f = 0.68$; IR (KBr pellet) 3175, 3094, 2856, 2362, 2337, 1541, 1429 cm^{-1}; H NMR (DMSO-d_6) 7.54 (1H, d, $J = 8.4$ Hz, aromatic proton), 7.07 (1H, d, $J = 8.4$ Hz, aromatic proton), 7.35 (1H, s, aromatic proton), 4.25 (2H, t, $J = 6$ Hz, methylene proton), 3.35 (2H, t, $J = 6$ Hz, methylene proton), 3.33(1H, s, hydroxyl proton), 2.42 (3H, s, methyl proton); MS (EI mode) *m*/*z* 201 (M^+), 171 ($M^+ - NO$); Anal. ($C_{11}H_{11}N_3O$) C, H, N.

The hydroxyimine product was reduced to **3-amino-2,3-dihydro-7-methyl-1*H*-pyrrolo[1,2-a]benzimidazole** by the following procedure: A mixture consisting of 800 mg of 3-hydroxylimine-2,3-dihydro-7-methyl-1*H*-pyrrolo[1,2-*a*]benzimidazole, 240 mL of methanol, and 800 mg of 5% Pd/charcoal catalyst was shaken at 50 psi H_2 for 48 h. Upon completion, the reaction mixture was opened to the air and filtered through a thin pad of Celite. The solvent was evaporated under reduced pressure. To the residue was added a little water, and the resulting solution was neutralized with saturated NaOH solution until basic (pH = 10 or 11). This solution was extracted 3× with 50 mL portions of chloroform and then the extracts were dried over Na_2SO_4. The solvent was evaporated under reduced pressure and the product was recrystallized from chloroform/hexane: 558 mg (75% yield); mp 100−102 °C; TLC [methanol/chloroform (1:9)] $R_f = 0.16$; IR (KBr pellet) 3337, 3273, 2914, 2361, 2337, 1520, 1460 cm^{-1}; ^1H NMR ($CDCl_3$) 7.60 (1H, d, $J = 8.1$ Hz, aromatic proton), 7.05 (1H, d, $J = 8.1$ Hz, aromatic proton), 7.11 (1H, s, aromatic proton), 4.20 and 4.01 (2H, m, methylene proton), 3.06 and 2.39 (2H, m, methylene proton), 4.52 (1H, t, $J = 7.2$ methine proton), 2.47 (3H, s, methyl proton). The spectral properties of this product agreed with those of the chiral product previously reported. Conversion of 3-amino-2,3-dihydro-7-methyl-1*H*-pyrrolo[1,2-*a*]benzimidazole to **2** was carried out as previously reported for the pure enantiomer.[5]

Procedure for Coupling 2 to Carboxylic Acids To Afford 1a−d. To a solution (1.00 mmol) of the carboxylic acid in 1.2 mL of anhydrous dichloromethane at 0 °C was added (1.10 mmol) 1,3-dicyclohexylcarodiimide (DCC) under a nitrogen atmosphere. The resulting mixture was stirred at 0 °C for 5 min, followed by addition (0.75 mmol) of **2** in 5 mL of anhydrous dichloromethane. The resulting mixture was then stirred at room temperature for 4 h. The *N*,*N*′-dicyclohexyl urea (DCU) was filtered off and the filtrate was dried over Na_2SO_4. Concentration of the filtrate afforded a red residue that was purified by preparative silica gel TLC.

6-Aziridinyl-2,3-dihydro-3-isonicotinamido-7-methyl-1*H*-pyrrolo[1,2-a]benzimidazole-5,8-dione (1a) was purified by preparative TLC using a mixture of 1% methanol and chloroform as solvent: 8 mg (37.9% yield); mp 160−162 °C; TLC [chloroform/methanol (90:10)] $R_f = 0.16$; IR (KBr pellet) 3445, 2361, 2337, 1674, 1637, 1521, 1313 cm^{-1}; ^1H NMR ($CDCl_3$) 8.67 (2H, d, $J = 6.8$ Hz, aromatic proton), 7.75 (2H, d, $J = 6.8$ Hz, aromatic proton), 8.96 (1H, d, $J = 5.7$ Hz, amide proton), 4.39 and 4.17 (2H, 2m, methylene proton), 5.34 (1H, m, 3-methine), 3.22 and 2.84 (2H, 2m, methylene proton), 2.36 (4H, s, aziridinyl protons), 1.99 (3H, s, 7-methyl); MS (EI mode) *m*/*z* 363 (M^+), 257 ($M^+ - COC_5H_4N$), 231. Anal. ($C_{19}H_{17}N_5O_3$) C, H, N.

(*R*)-6-Aziridinyl-2,3-dihydro-3-isonicotinamido−7-methyl-1*H*-pyrrolo[1,2-a]benzimidazole-5,8-dione ((*R*)-1a) was purified by preparative TLC using a mixture of 1% methanol and chloroform as solvent: 7 mg (19.6% yield); mp 162−165 °C; TLC [chloroform/methanol (90:10)] $R_f = 0.17$; IR (KBr pellet) 3445, 2361, 2337, 1674, 1637, 1521, 1314 cm^{-1}; ^1H NMR ($CDCl_3$) 8.67 (2H, d, $J = 6.8$ Hz, aromatic proton), 7.76 (2H, d, $J = 6.8$ Hz, aromatic proton), 9.04 (1H, d, $J = 5.7$ Hz, amide proton), 4.31 and 4.14 (2H, 2m, methylene proton), 5.29 (1H, m, 3-methine), 3.15 and 2.83 (2H, 2m, methylene proton), 2.39 (4H, s, aziridinyl protons), 1.99 (3H, s, 7-methyl); MS (EI mode) *m*/*z* 363 (M^+), 257 ($M^+ - COC_5H_4N$), 231. Anal. ($C_{19}H_{17}N_5O_3$) C, H, N.

(*S*)-6-aziridinyl-2,3-dihydro-3-isonicotinamido-7-methyl-1*H*-pyrrolo[1,2-a]benzimidazole-5,8-dione ((*S*)-1a) was purified by preparative TLC using a mixture of 1% methanol and chloroform as solvent. 5.6 mg (22% yield); mp 163−165 °C; TLC [chloroform/methanol (90:10)] $R_f = 0.18$; IR (KBr pellet) 3445, 2361, 2337, 1674, 1637, 1521, 1314 cm^{-1}; ^1H NMR ($CDCl_3$) 8.69 (2H, d, $J = 6.8$ Hz, aromatic proton), 7.74 (2H, d, $J = 6.8$ Hz, aromatic proton), 8.87 (1H, d, $J = 5.7$ Hz, amide proton), 4.45 and 4.15 (2H, 2m, methylene proton), 5.32 (1H, m, 3-methine), 3.21 and 2.83 (2H, 2m, methylene proton), 2.39 (4H, s, aziridinyl protons), 1.99 (3H, s, 7-methyl); MS (EI mode) *m*/*z* 363 (M^+), 257 ($M^+ - COC_5H_4N$), 231. Anal. ($C_{19}H_{17}N_5O_3$) C, H, N.

6-Aziridinyl-2,3-dihydro-7-methyl-3-(4-pyridylacetamido)-1*H*-pyrrolo[1,2-a]benzimidazole-5,8-dione (1b) was purified by preparative TLC plate using a solution of 3% methanol in chloroform as solvent: 7.5 mg (57% yield); mp 193−195 °C dec; TLC [chloroform/methanol (90:10)] $R_f = 0.166$; IR (KBr pellet) 3429, 2361, 2337, 1674, 1635, 1520, 1311 cm^{-1}; ^1H NMR ($CDCl_3$) 8.51 (2H, d, $J = 6.0$ Hz, aromatic proton), 7.24 (2H, d, $J = 6.0$ Hz, aromatic proton), 3.58 (2H, s, methylene proton), 8.09 (1H, d, $J = 5.7$ Hz, amide proton), 4.32 and 4.11 (2H, 2m, methylene proton), 5.29 (1H, m, 3-methine), 3.14 and 2.66 (2H, 2m, methylene proton), 2.37 (4H, s, aziridinyl protons), 1.98 (3H, s, 7-methyl); MS (EI mode) *m*/*z* 377 (M^+), 257 ($M^+ - COCH_2C_5H_4N$). Anal. ($C_{20}H_{19}N_5O_3$) C, H, N.

6-Aziridinyl-2,3-dihydro-7-methyl-3-nicotinicamido-1*H*-pyrrolo[1,2-a]benzimidazole-5,8-dione (1c) was purified by preparative TLC using a solution of 3% methanol in chloroform as solvent to yield 5.1 mg of title compound (52% yield): mp 168−170 °C dec; TLC [chloroform/methanol (90:10)] $R_f = 0.19$; IR (KBr pellet) 3431, 2361, 2337, 1645, 1521, 1313 cm^{-1}; ^1H NMR ($CDCl_3$) 9.17 (1H, s, aromatic proton), 8.71 (1H, d, $J = 6.9$ Hz, aromatic proton), 8.20 (1H, d, $J = 6.9$ Hz, aromatic proton), 7.36 (1H, m, aromatic proton), 8.86 (1H, d, $J = 5.7$ Hz, amide proton), 4.39 and 4.16 (2H, 2m, methylene proton), 5.34 (1H, m, 3-methine), 3.17 and 2.83 (2H, 2m, methylene proton), 2.37 (4H, s, aziridinyl protons), 1.99 (3H, s, 7-methyl); MS (EI mode) *m*/*z* 363 (M^+), 257 ($M^+ - COC_5H_4N$), 106. Anal. ($C_{19}H_{17}N_5O_3$) C, H, N.

6-Aziridinyl-2,3-dihydro-3-(4-quinolinecarboxamido)-7-methyl-1*H*-pyrrolo[1,2-a]benzimidazole-5,8-dione (1d) was purified by preparative TLC using a solution of 3% methanol in chloroform as solvent: 9 mg (37.5% yield); mp 152−154 °C dec; TLC [chloroform/methanol (90:10)] $R_f = 0.27$; IR (KBr pellet) 3437, 2361, 2337, 1653, 1521, 1315 cm^{-1}; ^1H NMR ($CDCl_3$) 8.94 (1H, d, $J = 8.1$ aromatic proton), 8.34 (1H, d, $J = 8.1$ Hz, aromatic proton), 8.13 (1H, d, $J = 8.1$ Hz, aromatic proton), 7.67 (1H, d, $J = 8.1$ Hz, aromatic proton), 7.75 (1H, m, aromatic proton), 7.58 (1H, m, aromatic proton), 8.45 (1H, d, $J = 5.7$ Hz, amide proton), 4.45 and 4.18 (2H, 2m, methylene proton), 5.35 (1H, m, 3-methine), 3.29 and 2.88 (2H, 2m, methylene proton), 2.340 (4H, s, aziridinyl protons), 1.989

(3H, s, 7-methyl); MS (EI mode) *m*/*z* 413 (M^+), 257 ($M^+ - COC_9H_7N$). Anal. ($C_{23}H_{19}N_5O_3$) C, H, N.

Procedure for Coupling 2 to Carboxylic Acids To Afford 1e,f. To a solution of 0.75 mmol of **2** in 0.5 mL of distilled pyridine, cooled with an ice−salt bath under a nitrogen atmosphere, was added 0.75 mmol of acid chloride. The mixture was stirred for 20 min with continued cooling. Water (∼5 mL) was added to the chilled reaction followed by extraction (3×) with 10-mL portions of chloroform. The extracts were dried over sodium sulfate and filtered, and the solvent was removed under reduced pressure. Product was purified by preparative TLC (1% methanol and chloroform) and recrystallized from chloroform/hexane.

6-Aziridinyl-2,3-dihydro-7-methyl-3-propanamido-1*H*-pyrrolo[1,2-a]benzimidazole-5,8-dione (1d): 30% yield; mp 190−193 °C dec; TLC [chloroform/methanol (90:10)] $R_f = 0.3$; IR (KBr pellet) 3421, 2926, 2361, 2337, 1674, 1520, 1311 cm^{-1}; ^1H NMR ($CDCl_3$) 2.36 (2H, q, $J = 7.3$ Hz, methylene proton), 1.15 (3H, t, $J = 7.3$ Hz, methylene proton), 8.63 (1H, d, $J = 5.7$ Hz, amide proton), 4.36 and 4.14 (2H, 2m, methylene proton), 5.27 (1H, m, 3-methine), 3.18 and 2.64 (2H, 2m, methylene proton), 2.34 (4H, s, aziridinyl protons), 1.99 (3H, s, 7-methyl); MS (EI mode) *m*/*z* 314 (M^+), 257 ($M^+ - COCH_2CH_3$), 243, 230. Anal. ($C_{16}H_{18}N_4O_3$) C, H, N.

3-Valerylamide-6-aziridinyl-2,3-dihydro-7-methyl-1*H*-pyrrolo[1,2-a]benzimidazole-5,8-dione (1f): 30% yield; mp 179−182 °C dec; TLC [chloroform/methanol (90:10)] $R_f = 0.39$; IR (KBr pellet) 3429, 2958, 2361, 2337, 1683, 1520, 1311 cm^{-1}; ^1H NMR ($CDCl_3$) 2.24 (2H, t, $J = 7.2$ Hz, methylene proton), 1.57 (2H, m, methylene proton), 1.33 (2H, m, methylene proton), 0.90 (3H, t, $J = 7.2$ Hz, methylene proton), 6.97 (1H, d, $J = 5.7$ Hz, amide proton), 4.45 and 4.13 (2H, 2m, methylene proton), 5.21 (1H, m, 3-methine), 3.22 and 2.58 (2H, 2m, methylene proton), 2.36 (4H, s, aziridinyl protons), 2.02 (3H, s, 7-methyl); MS (EI mode) *m*/*z* 342 (M^+), 257 ($M^+ - COCH_2CH_2CH_2CH_3$), 230. Anal. ($C_{18}H_{22}N_4O_3 \cdot 0.55H_2O$) C, H, N.

General Synthesis of 1-Monopeptide. To a solution (1.00 mmol) of tBOC-amino-protected l-amino acid in anhydrous dichloromethane was added (1.10 mmol) 1,3-dicyclohexylcarodiimide (DCC) in 1.2 mL of anhydrous dichloromethane at 0 °C. The resulting mixture was stirred at 5 °C for 5 min. To this solution was added (0.75 mmol) **3** in 5 mL of anhydrous dichloromethane, and the resulting mixture was stirred at room temperature for 1 h. The white solid residue was filtered off and 4 mL of trifluoroacetic acid was added to the solution at 5 °C and the mixture stirred at this temperature for 1.2 h. The solvent was removed and product was purified by reverse phase chromatography employing H_2O/acetonitrile (80:20) as the eluant (product either capped or converted to dipeptide at this point). The solid residue was then dissolved in a suspension of 80 mg of 5% Pd on charcoal in 35 mL of methanol and hydrogenated under 50 psi for 2 h. The solution was then filtered through Celite and concentrated to a dry residue consisting of the nitro-reduced (amino) derivative. A solution consisting of 80 mL of water and 800 mg of potassium phosphate monobasic was added to the amino derivative, followed by addition of 600 mg of Fremy's salt. The resulting mixture was stirred at room temperature for 4 h. The solvent was removed in vacuo, purified by reverse phase chromatography employing H_2O/acetonitrile (80:20) as the eluant, and concentrated to the dry quinone derivative. To the quinone derivative was added 15 mL of anhydrous methanol followed by addition of 0.4 mL of aziridine. This reaction mixture was stirred at room temperature for 3 h. The methanol solvent was evaporated, and the red residue was purified by silica gel flash chromatography employing chloroform/methanol (91:9) as the eluant. Recrystallization from ethyl acetate and hexane afforded pure amino acid linked **1**.

General Synthesis of Capped 1-Monopeptide and 1-Dipeptide. The amino acid-linked **3** prepared above was added to a solution consisting of 1.20 mmol of DCC and 1.10 mmol of the appropriate carboxylic acid or tBOC-amino-protected L-amino acid, in anhydrous dichloromethane held at 5 °C. The resulting mixture was stirred at room temperature for 2 h, the solid residue was then filtered off, and the solvent was removed in vacuo. The solid residue was then reduced, Fremy-oxidized, and aziridinated as described above.

(3*S*)-6-Aziridinyl-2,3-dihydro-3-(L-lysinylamino)-7-methyl-1*H*-pyrrolo[1,2-a]benzimidazole-5,8-dione (1g): 41 mg (17% yield); mp 153−155 °C (dec); TLC [dichloromethane/methanol, (90:10)] $R_f = 0.25$; IR (KBr pellet) 3124, 1712, 1642, 1613, 1563, 1467, 1221, 1184 cm^{-1}; ^1H NMR ($CDCl_3$) 9.51 (1H, d, $J = 8.30$ Hz, amide proton), 5.28 (1H, m, C(3) proton), 4.31 (1H, m, C(1) methlyene proton), 4.14 (1H, m, C(1) methylene proton), 3.76 (1H, m, C(4) proton), 2.95 (2H, m, C(2) methylene protons), 2.74 (2H, q, $J = 8.40$ Hz, C(5) methylene protons), 2.29 (4H, s, aziridine protons), 1.92 (3H, s, methyl protons), 1.74 (2H, m, C(8) methylene protons), 1.56 (2H, m, $J = 6.00$ Hz, C(6) methylene protons), 1.42 (2H, m, $J = 8.9$ Hz, C(7) methylene protons). Anal. ($C_{19}H_{26}N_6O_3$) C, H, N.

(3*S*)-6-Aziridinyl-2,3-dihydro-(glycinylamino)-7-methyl-3-1*H*-pyrrolo[1,2-a]benzimidazole-5,8-dione (1h): 38 mg (19% yield); mp 157−159 °C (dec); TLC [dichloromethane/methanol (90:10)] $R_f = 0.31$; IR (KBr pellet) 3295, 1704, 1685, 1643, 1505, 1289, 1156, 1081 cm^{-1}; ^1H NMR ($CDCl_3$) 8.53 (1H, d, $J = 8.06$ Hz, amide proton), 5.19 (1H, t, $J = 7.54$ Hz, C(3) proton), 4.23 (1H, m, C(1) methylene proton), 4.05 (1H, m, C(1) methylene proton), 3.10 (2H, s, (C4) methylene protons), 2.96 (1H, m, C(2) methylene proton), 2.41 (1H, m, C(2) methylene proton), 2.28 (4H, s, aziridine protons), 1.93 (3H, s, methyl protons). Anal. ($C_{15}H_{17}N_5O_3$) C, H, N.

(3*S*)-6-Aziridinyl-2, 3-dihydro-7-methyl-3-(L-prolinylamino)-1*H*-pyrrolo[1,2-a]benzimidazole-5,8-dione (1i): 44 mg (20% yield); mp 160−162 °C (dec); TLC [dichloromethane/methanol (90:10)] $R_f = 0.40$; IR (KBr pellet) 3034, 1721, 1675, 1656, 1478, 1239, 1183, 1121 cm^{-1}; ^1H NMR ($CDCl_3$) 8.59 (1H, broad, amide proton), 5.18 (1H, t, $J = 7.85$ Hz, C(3) proton), 4.42 (1H, m, C(1) methylene proton), 4.18 (1H, m, C(1) methylene proton), 3.85 (1H, dd, $J = 2.34$ Hz, $J = 7.36$ Hz (C4) proton), 3.18 (2H, m, C(7) methylene protons), 2.91 (1H, m, C(5) methylene proton), 2.53 (1H, m, C(5) methylene proton), 2.34 (4H, s, aziridine protons), 2.20 (1H, m, C(2) methylene proton), 2.05 (3H, s, methyl protons), 1.86 (1H, m, C(2) methylene proton), 1.75 (2H, q, $J = 8.45$ Hz, C(6) methylene protons). Anal. ($C_{18}H_{21}N_5O_3$) C, H, N.

(3*S*)-6-Aziridinyl-2,3-dihydro-3-(*N*-glycinyl-L-prolinylamino)-7-methyl-1*H*-pyrrolo[1,2-a]benzimidazole-5,8-dione (1j): 41 mg (16% yield); mp 169−171 °C (dec); TLC [dichloromethane/methanol (90:10)] $R_f = 0.15$; IR (KBr pellet) 3124, 1707, 1686, 1645, 1624, 1511, 1438, 1234, 1091 cm^{-1}; ^1H NMR ($CDCl_3$) 7.29 (1H, broad, amide proton), 4.43 (1H, q, $J = 8.10$ Hz, C(3) proton), 4.34 (1H, m, C(1) methlyene proton), 4.13 (1H, m, C(1) methlyene proton), 3.05 (1H, m, (C2) methlyene proton), 2.40 (1H, m, C(2) methlyene proton), 2.35 (4H, s, aziridine protons), 2.06 (3H, s, methyl protons), 1.68 (4H, s, C(6,7) methylene protons), 0.87 (2H, q, $J = 7.80$ Hz, C(5) methylene protons). Anal. ($C_{20}H_{24}N_6O_4$) C, H, N.

(3*S*)-6-Aziridinyl-2,3-dihydro-7-methyl-3-[*N*-(nicotinyl)-glycinylamino]-1*H*-pyrrolo[1,2-a]benzimidazole-5,8-dione (1k): 42 mg (15% yield); mp 168−170 °C (dec); TLC [dichloromethane/methanol (90:10)] $R_f = 0.42$; IR (KBr pellet) 3220, 1723, 1634, 1612, 1526, 1286, 1186 cm^{-1}; ^1H NMR ($CDCl_3$) 8.96 (1H, d, $J = 1.50$ Hz, aromatic proton), 8.53 (1H, q, $J = 1.20$ Hz, aromatic proton), 8.38 (1H, t, $J = 7.40$ Hz, amide proton), 8.17 (1H, d, $J = 7.80$ Hz, aromatic proton), 8.01 (1H, d, $J = 8.70$ Hz, amide proton), 7.22 (1H, q, $J = 4.80$ Hz, aromatic proton), 5.49 (1H, m, C(3)), 4.66 (1H, dd, $J = 7.20$ Hz, $J = 7.50$ Hz, C(4)), 4.24 (1H, m, $J = 4.50$ Hz, C(1) methylene proton), 4.17 (1H, m, $J = 7.20$ Hz, C(4) proton), 3.98 (1H, m, $J = 4.70$ Hz, C(1)), 3.10 (1H, m, C(2) methylene proton), 2.69 (1H, m, C(2) methylene proton), 2.21 (4H, t, $J = 7.80$ Hz, aziridine protons), 2.04 (3H, s, methyl protons). Anal. ($C_{21}H_{20}N_6O_4$) C, H, N.

(3*S*)-6-Aziridinyl-2,3-dihydro-7-methyl-3-(L-phenylalanylamino)-1*H*-pyrrolo[1,2-a]benzimidazole-5,8-dione (1l): 40 mg (18% yield); mp 163−165 °C (dec); TLC [dichloromethane/methanol (90:10)] $R_f = 0.36$; IR (KBr pellet) 3387, 1674, 1637, 1518, 1311, 1138, 1031 cm^{-1}; ^1H NMR ($CDCl_3$) 8.13

(1H, d, J = 8.21 Hz, amide proton), 7.31 (2H, m, aromatic protons), 7.24 (1H, m, aromatic proton), 7.20 (2H, m, aromatic protons), 5.23 (1H, q, J = 7.50 Hz, C(3) proton), 4.37 (1H, m, C(1) methylene proton), 4.17 (1H, m, C(1) methylene proton), 3.70 (1H, dd, J = 5.50 Hz, J = 2.10 Hz, C(4) proton), 3.21 (1H, dd, J = 4.01 Hz, J = 4.01 Hz, C(5) methylene proton), = 2.76 (1H, dd, J = 9.50 Hz, J = 4.00 Hz, C(5) methylene proton), 3.15 (1H, m, C(2) methylene proton), 2.49 (1H, m, C(2) methylene proton), 2.34 (4H, s, aziridine), 2.05 (3H, s, methyl protons). Anal. ($C_{22}H_{23}N_5O_3$) C, H, N.

(3*S*)-6-Aziridinyl-2,3-dihydro-7-methyl-1*H*-3-(*N*-L-phenylalanyl-L-phenylalanylamino)-pyrrolo[1,2-a]benzimidazole-5,8-dione (1m): 51 mg (15% yield); mp 173−175 °C (dec); TLC [dichloromethane/methanol (90:10)] R_f = 0.51; IR (KBr pellet) 3144, 1702, 1682, 1643, 1523, 1513, 12451, 1124 cm^{-1}; ^1H NMR ($CDCl_3$) 7.96 (1H, broad, amide proton), 7.30 (5H, m, J = 7.50 Hz, aromatic protons), 7.17 (5H, m, J = 7.50 Hz, aromatic protons), 5.12 (1H, broad, amide proton), 4.78 (1H, q, J = 7.34 Hz, C(3) proton), 4.29 (1H, m, C(1) methylene proton), 4.18 (1H, m, C(1) methylene proton), 4.05 (2H, d, J = 6.90 Hz, methylene protons), 3.47 (2H, d, J = 7.00 Hz, methylene protons), 3.23 (1H, q, J = 6.00 Hz, C(4) proton), 3.17 (1H, m, J = 7.20 Hz, C(5) proton), 3.09 (1H, m, C(2) methylene proton), 2.61 (1H, m, C(2) methylene proton), 2.35 (4H, s, aziridine protons), 2.01(3H, s, methyl protons). Anal. ($C_{31}H_{32}N_6O_4$) C, H, N.

(3*S*)-6-Aziridinyl-2,3-dihydro-7-methyl-3-(D-phenylalanylamino)-1*H*-pyrrolo[1,2-a]benzimidazole-5,8-dione (1n): 12% yield; mp 157−159 °C (dec); TLC [dichloromethane/methanol (90:10)] R_f = 0.4; IR (KBr pellet) 3380, 2924,1674, 1637, 1518 cm^{-1}; ^1H NMR ($CDCl_3$) 8.02 (1H, d, J = 6.1 Hz, amide proton), 7.22 (5H, m, aromatic protons), 5.16 (1H, m, methine proton), 4.40 (1H, m, methylene proton), 4.22 (1H, m, methylene proton), 3.60 (1H, m, methylene proton), 3.15 (1H, m, methylene proton), 3.28 (1H, dd, J = 2.4 Hz methine proton), 2.72 (1H, m, methylene proton), 2.51 (1H, m, methylene proton), 2.35 (4H, s, aziridinyl protons), 2.06 (3H, s, methyl protons). Anal. ($C_{22}H_{23}N_5O_3 \cdot 1.1H_2O$) C, H, N; calcd H, 5.96; found H, 5.46.

Cleavage of ^{32}P-End-Labeled DNA. ^{32}P-end-labeled 514 base pair restriction fragments were prepared by first digesting supercoiled pBR322 plasmid DNA with *Eco*R I restriction endonuclease. For 3′-end labeling, terminal deoxynucletidyl transferase and [α-^{32}P]dATP were used to incorporate the ^{32}P-end. 5′-end labeling was achieved by the treatment of the *Eco*R I pre-cleaved DNA with alkaline phosphatase, [γ-^{32}P]ATP and T4 polynucleotide kinase. Following the end-labeling, the DNA was further digested with *Rsa* I to yield the 514 base pair fragment that was purified by 6% preparative nondenaturing gel electrophoresis.

PBI-induced cleavage reactions were carried out in 20 μL total volumes containing calf thymus DNA (40 or 50 μM nucleotide concentration), 2×10^4 cpm ^{32}P-end-labeled restriction fragment, and various concentrations of drugs in DMSO in 50 mM phosphate buffer (pH 7.4). Reaction mixtures were degassed under argon for 5 min before being initiated by the addition of 1 mM of sodium dithionite. The reactions were quenched after 5 min through ethanol precipitation in the presence of 0.3 M sodium acetate. The DNA pellet was washed with 70% ethanol, dried, and resuspended in 3 μL of either 80% foramide loading dye or NaOH loading dye. Piperidine treatment was also carried out by dissolving the DNA pellet in 20 μL of freshly prepared 0.2 M piperidine, heatimg at 90 °C for 10 min, and drying.

Preparation of the PBI−DNA Adducts. The PBI−DNA adduct was prepared by mixing 4.0 mg (1.0 μmol of strand) of calf thymus DNA in 0.05 M of Tris buffer (pH 7.4) with 4.0 mg (16 μmol) of the PBI in 0.25 mL of DMSO. To the mixture was added 2 mg of 5% Pd on C. The resulting mixture was degassed under argon for 30 min, followed by purging with H_2 for 10 min. The mixture was then purged with argon for 10 min and incubated at 30 °C for 24 h. The reaction was opened to the air and the catalyst was syringe-filtered off. To the filtrate were added 0.45 mL of 7.5 M ammonium acetate and 10 mL of cold ethanol, and the mixture was left in a −20 °C freezer for 24 h. The mixture was centrifuged at 14 000*g* for 20 min and the supernatant was removed. The DNA pellet was redissolved in water, ethanol precipitated, and dried. The dried pellet was weighed and dissolved in 1 mL of double distilled water resulting in a clear solution with $\lambda_{max} \sim 550$ nm, $\epsilon \sim 750$ M^{-1} cm^{-1} . This is the chromophore of the aminoquinone resulting from nucleophile-mediated opening of the aziridine ring.

Molecular Modeling. The models of interactions between reduced **1** and the major groove of DNA were constructed with Insight II software (Accelrys Inc). A B-form duplex DNA model of the sequence where cleavage was observed in PAGE gels (3-GGTAATAATAG-5) was made using the Biopolymer Module. A minimized structure (cvff.frc force field, steepest descent, 1000 iterations) of reduced **1** was linked to the phosphate oxygen where the PAGE indicated that hydrolytic cleavage had occurred. Linkage of the aziridinyl group to the phosphate oxygen was carried out by converting the aziridinyl group to an aminoethyl group and then creating a bond between the methyl of the aminoethyl group and the phosphate oxygen, resulting in a $-NHCH_2CH_2O-$ linkage. The resulting DNA adduct was minimized while all heavy atoms were constrained and only hydrogen atoms were allowed to move. The linked reduced **1** was docked into the major groove by setting upper and lower bond distances for hydrogen-bond distances (1.8−1.5 Å) between reduced **1** and the AT base pair (see Figure 1) and mimimizing while all DNA atoms were constrained and reduced **1** was allowed to move (cvff.frc force field, steepest descent, 1×10^6 iterations, derivative = 0.001). This process was repeated while all DNA atoms were constrained except those of the base pairs where interactions with reduced **1** occurred.

Acknowledgment. We thank the National Institutes of Health, National Science Foundation, and the Arizona Disease Control Research Commission for their generous support.

References

(1) Schulz, W. G.; Islam, E.; Skibo, E. B. Pyrrolo[1,2-*a*]benzimidazole-Based Quinones and Iminoquinones. The Role of the 3-Substituent on Cytotoxicity. *J. Med. Chem.* **1995**, *38*, 109−118.
(2) Schulz, W. G.; Nieman, R. A.; Skibo, E. B. Evidence for DNA Phosphate Backbone Alkylation and Cleavage by Pyrrolo[1,2-*a*] benzimidazoles, Small Molecules Capable of Causing Sequence Specific Phosphodiester Bond Hydrolysis. *Proc. Natl. Acad. Sci. U.S.A.* **1995**, *92*, 11854−11858.
(3) Skibo, E. S.; Gordon, S.; Bess, L.; Boruah, R.; Heileman, J. Studies of Pyrrolo[1,2-*a*]benzimidazole Quinone DT-Diaphorase Substrate Activity, Topoisomerase II Inhibition Activity, and DNA Reductive Alkylation. *J. Med. Chem.* **1997**, *40*, 1327−1339.
(4) Skibo, E. B. Pyrrolobenzimidazoles in cancer treatment. *Expert. Opin. Ther. Patents* **1998**, *8*, 673−701.
(5) Craigo, W. A.; LeSueur, B. W.; Skibo, E. B. Design of Highly Active Analogues of the Pyrrolo[1,2-a]benzimidazole Antitumor Agents. *J. Med. Chem.* **1999**, *42*, 3324−3333.
(6) Huang, X.; Suleman, A.; Skibo, E. B. Rational Design of Pyrrolo-[1,2-*a*]benzimidazole Based Antitumor Agents Targeting the DNA Major Groove. *Bioorg. Chem.* **2000**, *28*, 324−337.
(7) Skibo, E. B.; Schulz, W. G. Pyrrolo[1,2-*a*]benzimidazole-Based Aziridinyl Quinones. A New Class of DNA Cleaving Agent Exhibiting G and A Base Specificity. *J. Med. Chem.* **1993**, *36*, 3050−3055.
(8) Komiyama, M.; Sumaoka, J. Progress towards synthetic enzymes for phosphoester hydrolysis. *Curr. Opin. Chem. Biol.* **1998**, *2*, 751−757.
(9) Franklin, S. J. Lanthanide-mediated DNA hydrolysis. *Curr. Opin. Chem. Biol.* **2001**, *5*, 201−208.
(10) Jubian V.; Dixon, R. P.; Hamilton, A. D. Molecular Recognition and Catalysis. Acceleration of Phosphodiester Cleavage by a Simple Hydrogen-Bonding Receptor. *J. Am. Chem. Soc.* **1992**, *114*, 1120−1121.
(11) Schatzlein, A. G.; Rutherford, C.; Corrihons, F.; Moore, B. D. Phage derived peptides for targeting of doxorubicin conjugates to solid tumors. *J. Controlled Release* **2001**, *74*, 357−362.
(12) Janaky, T.; Juhasz, A.; Bajusz, S.; Csernus, V.; Srkalovic, G.; Bokser, L.; Milovanovic, S.; Redding, T. W.; Rekasi, Z.; Nagy, A.; Schally, A. V. Analogues of Luteinizing-Hormone-Releasing Hormone Containing Cytotoxic Groups. *Proc. Natl. Acad. Sci. U.S.A.* **1992**, *89*, 972−976.

(13) Sheh, L.; Chang, H. W.; Ong, C. W.; Chen, S. L.; Bailly, C.; Linssen, R. C. M.; Waring, M. J. Synthesis, Dna-Binding, and Sequence Specificity of Dna Alkylation by Some Novel Cyclic Peptide Chlorambucil Conjugates. *Anti-Cancer Drug Des.* **1995**, *10*, 373−388.
(14) Sheh, L. U.; Dai, H. Y.; Kuan, Y. H.; Li, C. J.; Chiang, C. D.; Cheng, V. Synthesis and Cytotoxicity Studies of Novel Cyclic Peptide-2,6-Dimethoxyhydroquinone-3-Mercaptoacetic Acid Conjugates. *Anti-Cancer Drug Des.* **1993**, *8*, 237−247.
(15) Samnick, S.; Schaefer, A.; Siebert, S.; Richter, S.; Vollmar, B.; Kirsch, C. M. Preparation and investigation of tumor affinity, uptake kinetic and transport mechanism of iodine-123-labeled amino acid derivatives in human pancreatic carcinoma and glioblastoma cells. *Nuclear Med. Biol.* **2001**, *28*, 13−23.
(16) Panov, V.; Salomon, Y.; Kabalka, G. W.; Bendel, P. Uptake and washout of borocaptate sodium and borono-phenylalanine in cultured melanoma cells: A multinuclear NMR study. *Radiat. Res.* **2000**, *154*, 104−112.
(17) Nemoto, H.; Cai, J.; Asao, N.; Iwamoto, S.; Yamamoto, Y. Synthesis and biological properties of water-soluble p-boronophenylalanine derivatives. Relationship between water solubility, cytotoxicity, and cellular uptake. *J. Med. Chem.* **1995**, *38*, 1673−1678.
(18) Skibo, E. B.; Islam, I.; Schulz, W. G.; Zhou, R.; Bess, L.; Boruah, R. The Organic Chemistry of the Pyrrolo[1,2-*a*]benzimidazole Antitumor Agents. An Example of Rational Drug Design. *Synlett* **1996**, 297−309.
(19) Xing, C.; Skibo, E. B.; Dorr, R. T. Aziridinyl Quinone Antitumor Agents based on Indoles and Cyclopent[b]indoles: Structure Activity Relationships for Cytotoxicity and Antitumor Activity. *J. Med. Chem.* **2001**, *44*, 3545−3562.
(20) Maxam, A. M.; Gilbert, W. Sequencing End-Labeled DNA with Base-Specific Chemical Cleavages. *Methods Enzymol.* **1980**, *65*, 499−560.
(21) Skibo, E. B.; Xing, C.; Groy, T. Recognition and Cleavage at the DNA Major Groove. *Bioorg. Med. Chem.* **2001**, *9*, 2445−2459.
(22) Paull, D. K.; Shoemaker, R. H.; Hodes, L.; Monks, A.; Scudiero, D. A.; Rubinstein, L.; Plowman, J.; Boyd, M. R. Display and Analysis of Differential Activity of Drugs Against Human Tumor Cell Lines: Development of Mean Graph and COMPARE Algorithm. *J. Natl. Cancer Inst.* **1989**, *81*, 1088−1092.
(23) Boyd, M. R. *Principles and Practices of Oncology (PPO updates)*; J. B. Lippincott: 1989.
(24) Suleman, A.; Skibo, E. B. Insights into the Mechanism and Substrate Specificty of Human DT-Diaphorase through Molecular Modeling. *J. Med. Chem.* **2002**, *45*, 1211−1220.
(25) Sausville, E. A.; Zaharevitz, D.; Gussio, R.; Meijer, L.; Louarn-Leost, M.; Kunick, C.; Schultz, R.; Lahusen, T.; Headlee, D.; Stinson, S.; Arbuck, S. G.; Senderowicz, A. Cyclin-Dependent Kinases: Initial Approaches to Exploit a Novel Therapeutic Target. *Pharmacol. Ther.* **1999**, *82*, 285−292.
(26) Li, H.; Hallows, W. H.; Punzi, J. S.; Marquez, V. E.; Carrell, H. L.; Pankiewicz, K. W.; Watanabe, K. A.; Goldstein, B. M. Crystallographic studies of two alcohol dehydrogenase-bound analogues of thiazole-4-carboxamide adenine dinucleotide (TAD), the active anabolite of the antitumor agent tiazofurin. *Biochemistry* **1994**, *33*, 23−32.
(27) Cappellacci, L.; Franchetti, P.; AbuSheikha, G.; Jayaram, H. N.; Gurudutt, V. V.; Sint, T.; Schneider, B. P.; Goldstein, B. M.; Perra, G.; Poma, S.; LaColla, P.; Grifantini, M. Synthesis and cytotoxic activity of selenophenfurin, a new inhibitor of IMP dehydrogenase. *Nucleosides Nucleotides* **1997**, *16*, 1045−1048.
(28) Franchetti, P.; Cappellacci, L.; AbuSheikha, G.; Jayaram, H. N.; Schneider, B. P.; Sint, T.; Gurudutt, V. V.; Collart, F. R.; Huberman, E.; Grifantini, M. Synthesis and IMP dehydrogenase (type I and type II) inhibitory activity of isosteric NAD analogues derived from thiophenfurin and furanfurin. *Nucleosides Nucleotides* **1997**, *16*, 1415−1418.
(29) Franchetti, P.; Cappellacci, L.; Perlini, P.; Jayaram, H. N.; Butler, A.; Schneider, B. P.; Collart, F. R.; Huberman, E.; Grifantini, M. Isosteric analogues of nicotinamide adenine dinucleotide derived from furanfurin, thiophenfurin, and selenophenfurin as mammalian inosine monophosphate dehydrogenase (type I and II) inhibitors. *J. Med. Chem.* **1998**, *41*, 1702−1707.
(30) Franchetti, P.; Cappellacci, L.; Grifantini, M. IMP Dehydrogenase as a Target of Antitumor and Antiviral Chemotherapy. *Farmaco* **1996**, *51*, 457−469.
(31) Szekeres, T.; Sedlak, J.; Novotny, L. Benzamide riboside, a recent inhibitor of inosine 5′-monophosphate dehydrogenase induces transferrin receptors in cancer cells. *Curr. Med. Chem.* **2002**, *9* (7), 759−764.
(32) Novotny, L.; Rauko, P.; Yalowitz, J. A.; Szekeres, T. Antitumor activity of benzamide riboside in vitro and in vivo. *Curr. Med. Chem.* **2002**, *9*, 773−779.
(33) Jager, W.; Salamon, A.; Szekeres, T. Metabolism of the novel IMP dehydrogenase inhibitor benzamide riboside. *Curr. Med. Chem.* **2002**, *9*, 781−786.
(34) Hissin, P. J.; Hilf, R. Characteristics of proline transport into *R*3230AC mammary tumor cells. *Biochim. Biophys. Acta* **1978**, *508*, 401−412.
(35) Morikawa, T.; Tada, K. Transport system common to imino acids and glycine. *Tohoku J. Exp. Med.* **1967**, *93*, 31−38.
(36) Goenner, S.; Boutron, A.; Soni, T.; Lemonnier, A.; Moatti, N. Amino acid transport systems in the human hepatoma cell line Hep G2. *Biochem Biophys. Res. Commun.* **1992**, *189*, 472−479.
(37) Uchino, H.; Kanai, Y.; Kim, D. K.; Wempe, M. F.; Chairoungdua, A.; Morimoto, E.; Anders, M. W.; Endou, H. Transport of amino acid-related compounds mediated by L-type amino acid transporter 1 (LAT1): Insights into the mechanisms of substrate recognition. *Mol. Pharmacol.* **2002**, *61*, 729−737.
(38) Schallreuter, K. U.; Wood, J. M. The Importance of L-Phenylalanine Transport and Its Autocrine Turnover to l-Tyrosine for Melanogenesis in Human Epidermal Melanocytes. Biochem. Biophys. Res. Commun. **1999**, *262*, 423−428.
(39) Jaffar, M.; Naylor, M. A.; Robertson, N.; Stratford, I. J. Targeting hypoxia with a new generation of indolequinones. *Anti. Cancer Drug. Des.* **1998**, *13*, 593−609.
(40) Phillips, R. M.; Naylor, M. A.; Jaffar, M.; Doughty, S. W.; Everett, S. A.; Breen, A. G.; Choudry, G. A.; Stratford, I. J. Bioreductive activation of a series of indolequinones by human DT-diaphorase: Structure−activity relationships. *J. Med. Chem.* **1999**, *42*, 4071−4080.

JM0302750